

All-optical switching in silicon photonic crystal waveguides by use of the plasma dispersion effect

Francis C. Ndi and Jean Toulouse

Department of Physics, Lehigh University, 16 Memorial Drive East, Bethlehem, Pennsylvania 18015

Tim Hodson and Dennis W. Prather

Department of Electrical & Computer Engineering, University of Delaware, Newark, Delaware 19711

Received February 3, 2005; revised manuscript received April 29, 2005; accepted May 17, 2005

Silicon photonic crystals offer new ways of controlling the propagation of light as well as new tools for the realization of high-density optical integration on monolithic substrates. However, silicon does not possess the strong nonlinearities that are commonly used in the dynamic control of optical devices. Such dynamic control is nevertheless essential if silicon is to provide the higher levels of functionality that are required for optical integration. We demonstrate that the combination of the refractive index change caused by the presence of photoexcited carriers, or so-called plasma dispersion, and photonic crystal properties such as photonic bandgaps, constitutes a powerful tool for active control of light in silicon integrated devices. We show close to 100% modulation depth near the photonic crystal band edge. © 2005 Optical Society of America
OCIS codes: 130.312, 230.1150.

High-density optical integration on a monolithic substrate is an ongoing concern for the photonics community, and silicon has been shown to be a substrate of choice for its realization.¹ This is partly due to the fact that silicon is transparent in the infrared region of the spectrum and also because it offers a well-developed fabrication technology. To achieve high levels of functionality in a silicon waveguide, one needs to actively or dynamically control the confinement and propagation of light in it. Unfortunately, silicon does not possess strong nonlinearities, such as those that are present in certain glasses or ferroelectric materials that are commonly used for active light control. One method used to perform active light control in silicon is the plasma dispersion effect,²⁻⁴ which involves changing the refractive index of silicon by the creation, injection, or depletion of charge carriers. However, many existing implementations generate charge carriers by electronic means such as through a p-i-n junction, which may be undesirable in certain applications and potentially slower compared with direct optical generation.

The plasma dispersion effect is particularly well suited to control of light in photonic crystal (PC) devices. This is because, unlike conventional waveguides, typical PC structures exhibit sharp transitions in their transmission spectra, especially near the band edges.⁵ In these regions of sharp transitions, small changes in the refractive index of the silicon host can lead to drastic changes in transmission properties. Almeida *et al.*⁶ have demonstrated the viability of using optically induced plasma dispersion in switching, using a ring resonator coupled to a waveguide operating at hundreds of megahertz. Leonard *et al.*⁷ have also shown optically induced ultrafast PC band-edge tuning. While these results show the promise of optically induced plasma dispersion in switching applications, there are still signifi-

cant challenges to address, especially with respect to carrier lifetime engineering and the adverse thermal effect of carrier cooling and recombination.

In this Letter we present both simulation and experimental results on the modulation of transmission in planar silicon PC waveguides making use of optically induced plasma dispersion. We show that a 100% modulation depth can be achieved near the transmission band edge. We also show that, in practical situations, at high power levels of the optical pump, adverse thermal effects from carrier cooling and recombination become significant and must be addressed.

The goal of the simulation was to examine the shift in the transmission spectrum due to photoexcited carriers in the silicon host. The excited carriers cause a reduction in the real part of the refractive index, which can be described approximately by the Drude free carrier dispersion equation²:

$$\Delta n_r = - \frac{e^2 \lambda^2}{8 \pi^2 c^2 \epsilon_0 n_o} \left(\frac{\Delta N_e}{m_e} + \frac{\Delta N_h}{m_h} \right), \quad (1)$$

where Δn_r is the change in the real part of the refractive index as a result of changes in the electron and hole concentrations, ΔN_e and ΔN_h , respectively; ϵ_0 is the permittivity of free space; e is the electron charge; n_o is the refractive index of the unperturbed silicon; m_e and m_h are effective masses of electrons and holes; and λ is the probe wavelength of interest.

Our PC waveguide was designed to have a transmission band edge near 1600 nm (shown by the solid curve in Fig. 1), which is the median wavelength of our tunable laser. The model assumed a 0.26 μm thick silicon layer on a 1 μm oxide base. The design process resulted in a triangular lattice of airholes with a diameter of 0.38 μm and a lattice spacing of

0.45 μm . The PC waveguide consisted of a missing row of nearest-neighbor holes. According to Eq. (1), an experimentally achievable change of $5 \times 10^{19} \text{ cm}^{-3}$ in carrier concentration results in a change of approximately -0.1 in refractive index at wavelengths close to 1550 nm. This reduction in the refractive index leads to a blueshift in the transmission spectrum,⁸ of approximately 50 nm, as indicated by the dashed curve in Fig. 1.

A PC waveguide was then fabricated on a silicon-on-insulator wafer with the same lattice parameters as in the simulation. Our experimental setup is shown in Fig. 2(a). The probe signal came from a tunable laser (1540–1660 nm), collimated and polarized such that the electric field was parallel to the plane of the PC lattice. It is for this orientation of the field that the PC waveguide has guiding properties.⁸ The probe was focused onto the straight edge of a 10 μm wide ridge waveguide ending in a parabolic reflector that focused the light into the PC waveguide. The output light from the PC waveguide was coupled to a single-mode fiber and onto a detector, using another parabolic mirror–ridge waveguide combination. The waveguide structure is shown as an inset in Fig. 2(b) and described in greater detail in Ref. 9. The scattered light due to mode mismatch at the input and output of the PC waveguide was used as a visual aid to image the transmission from above with an infrared camera. A dichroic mirror and microscope objective were used to focus the pump (808 nm diode la-

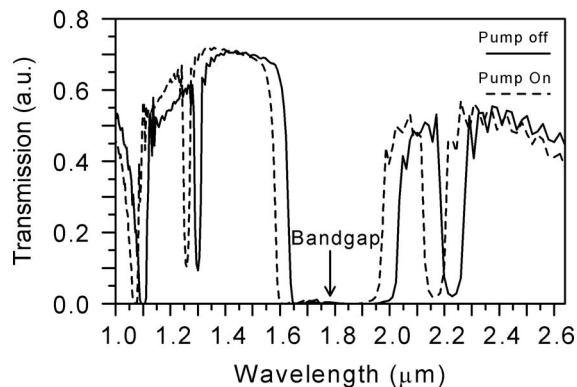


Fig. 1. Simulated transmission spectra of a sample with the pump off (solid curve) and the pump on (assuming a refractive index change of -0.1 , shown by the dashed curve).

ser) to a 100 μm spot on the surface of the sample, centered on the PC waveguide.

Figure 2(b) shows the transmission spectrum of our sample, indicating the beginning of a bandgap at 1610 nm. The drop in transmission at shorter wavelengths is not a property of the PC waveguide but is due to the fact that higher-order modes of the ridge waveguides tend to be excited at those wavelengths, leading to higher coupling losses at the input of the PC waveguide and at the ridge waveguide–fiber interface. However, since our focus is on the wavelengths close to the bandgap, this artifact does not affect our results or conclusions.

Figure 3 shows the effect of a continuous-wave pump at 808 nm on the transmission of the probe at 1601.8 nm. The probe was chosen to lie just to the left of the bandgap so that the expected blueshift from the Drude effect would result in a sharp drop in transmission. The pump was set at approximately 200 mW and turned on after 25 s. The data show a drop of 55% in the transmission of the probe with the pump on. The insets in Fig. 3 are pictures from the infrared camera showing the scattered probe light with the pump first off and then on. The dot of light at the lower output end of the PC waveguide is due to mode mismatch between the guided PC mode and the taper of the ridge waveguide when the light is transmitted through the waveguide. When the pump is turned on, this dot of light almost disappears, indicating that very little light is then being transmitted. The result in Fig. 3 for the continuous-wave pump was not time resolved because of the long averaging time (50 ms) of the detector used, so the data are more likely to include effects that are secondary to carrier generation such as thermal effects resulting from carrier cooling and recombination.

Figure 4 shows time-resolved measurements done on a second but similar sample using 3 ps pulses at 808 nm from a Ti:sapphire laser with a repetition rate of 76 MHz. The pulse energy was approximately 10 nJ, and the spot size on the sample was such that the concentration of carriers generated (approximately 10^{17} cm^{-3}) was small enough to minimize the effects of free carrier absorption. Although free carrier absorption might be a beneficial effect in this case as it would increase the overall modulation depth. The result was obtained with a 2.5 GHz pho-

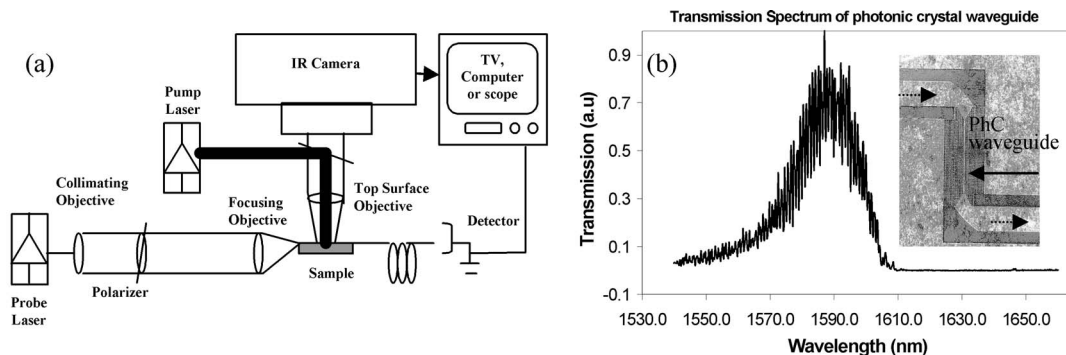


Fig. 2. (a) Top view of the experimental sample characterization setup. The plane of the PC is perpendicular to the paper. (b) Transmission spectrum of the sample. The plot shows beginning of a bandgap at 1610 nm. The inset shows a scanning electron microscope picture of the sample.

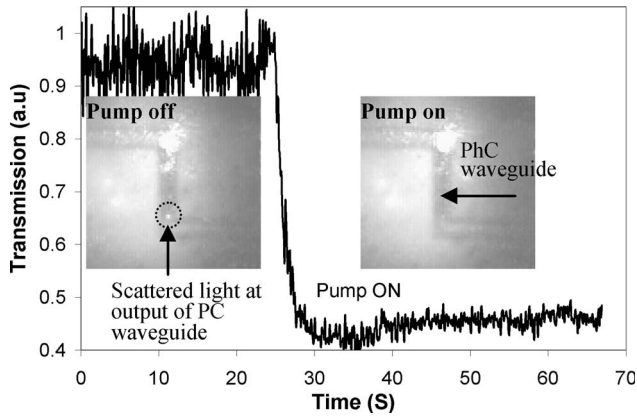


Fig. 3. Turning on the pump (200 mW at 808 nm) leads to a drop in transmission of the probe (at 1601.8 nm) due to plasma dispersion. The waveguide is shown with the pump off and on.

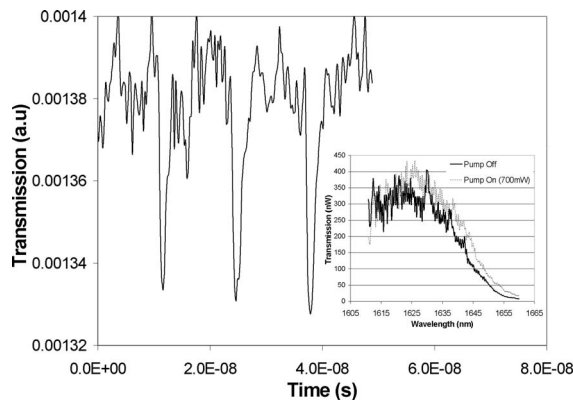


Fig. 4. Time-resolved measurement done on a second sample by use of 3 ps pulses at 808 nm from a Ti:sapphire laser with a repetition rate of 76 MHz. The data show a response of less than 2 ns to the 3 ps excitation. The inset shows a redshift in the transmission at high pump power associated with a thermo-optic effect from carrier cooling and recombination.

todiode connected to a fast oscilloscope triggered by the Ti:sapphire laser. The data show a response of less than 2 ns to the 3 ps pump excitation.

The inset in Fig. 4 shows a limited section of the transmission spectrum of our second sample (solid curve). The dotted curve in the inset shows a measured redshift in the transmission spectrum following excitation by a 700 mW continuous-wave pump at 808 nm. This redshift can be associated with a thermo-optic effect resulting from carrier cooling and

recombination,^{10–12} the effect of which is reinforced by the insulating oxide layer underneath the silicon device layer. We also observed (not shown) that the magnitude of the redshift increases with pump power and is also present as a background when the pump is pulsed. Clearly, this adverse redshift must be addressed in a practical application.

In conclusion, we have demonstrated optically induced modulation of the transmission in a planar silicon photonic crystal waveguide, using the plasma dispersion effect. The modulation depth can be as high as 100% close to the transmission band edge, which is where the transmission of the PC waveguide drops sharply to zero due to the presence of a bandgap. Thus, operation of the waveguide close to the band edge can allow for direct in-line modulation with a high modulation depth, which is not the case in structures such as Mach–Zehnder interferometers in which the beam must be split. We have also demonstrated that, for this modulation scheme to be practical, appropriate steps must be taken to minimize the thermal effects that result from hot carrier cooling and recombination and tend to cancel out the plasma dispersion effect.

F. C. Ndi's e-mail address is frn2@lehigh.edu.

References

1. L. Pavesi, *J. Phys. Condens. Matter* **15**, R1169 (2003).
2. R. A. Soref and B. R. Bennett, *IEEE J. Quantum Electron.* **QE-23**, 123 (1987).
3. C. A. Barrios, V. R. Almeida, R. Panepucci, and M. Lipson, *J. Lightwave Technol.* **21**, 2332 (2003).
4. S. R. Giguere, L. Friedman, R. A. Soref, and J. P. Lorenzo, *J. Appl. Phys.* **68**, 4964 (1990).
5. R. D. Meade, K. D. Brommer, A. M. Rappe, and J. D. Joannopoulos, *Phys. Rev. B* **44**, 13772 (1991).
6. V. R. Almeida, C. A. Barrios, R. R. Panepucci, M. Lipson, M. A. Foster, D. G. Ouzounov, and A. L. Gaeta, *Opt. Lett.* **29**, 2867 (2004).
7. S. W. Leonard, H. M. van Driel, J. Schilling, and R. B. Wehrspohn, *Phys. Rev. B* **66**, 161102(R) (2002).
8. J. D. Joannopoulos, R. D. Meade, and J. N. Winn, *Photonic Crystals: Molding the Flow of Light* (Princeton U. Press, 1995).
9. D. W. Prather, J. Murakowski, S. Shi, S. Venkataraman, A. Sharkawy, C. Chen, and D. Pustai, *Opt. Lett.* **27**, 1601 (2002).
10. M. C. Downer and C. V. Shank, *Phys. Rev. Lett.* **56**, 761 (1986).
11. J. M. Liu, H. Kurz, and N. Bloembergen, *Appl. Phys. Lett.* **41**, 643 (1982).
12. M. Bertolotti, A. Ferrari, C. Sibilis, and M. Tamburrini, *Appl. Phys. A Solids Surf.* **37**, 109 (1985).